

Short Communication

Intermediate Temperature Electrical Properties of a (Na/K)Ti₂(PO₄)₃/Ti_{0.9}Mg_{0.1}P₂O₇ Composite Electrolyte

Yongzhong Wang¹, Ruifeng Du¹, Wenli Hu², Hongtao Wang^{1,*}, Huiquan Li^{1,**}

¹ School of Chemical and Material Engineering, Fuyang Normal College; Anhui Provincial Key Laboratory for Degradation and Monitoring of Pollution of the Environment, Fuyang 236037, China

² Fuyang Preschool Education College, Fuyang 236037, China

*E-mail: hongtaoking3@163.com, huiquanli0908@163.com

Received: 9 April 2018 / Accepted: 22 May 2018 / Published: 5 June 2018

In this paper, a composite electrolyte of (Na/K)Ti₂(PO₄)₃/Ti_{0.9}Mg_{0.1}P₂O₇ was synthesized using Ti_{0.9}Mg_{0.1}P₂O₇ and NaCl/KCl as raw materials. The composite electrolyte was characterized with XRD, SEM and EIS. The result of X-ray diffraction (XRD) indicated that an *in-situ* reaction fully occurred to Mg²⁺-doped titanium pyrophosphate and inorganic molten salt to form the Ti_{0.9}Mg_{0.1}P₂O₇ and (Na/K)Ti₂(PO₄)₃ bimorph structure. It can be seen from scanning electron microscopy (SEM) images that Ti_{0.9}Mg_{0.1}P₂O₇ and (Na/K)Ti₂(PO₄)₃ are fused each other. The electrical conductivities results by electrochemical impedance spectroscopy (EIS) indicated that the (Na/K)Ti₂(PO₄)₃/Ti_{0.9}Mg_{0.1}P₂O₇ shows a greatly improvement of conductivities. Finally, an H₂/O₂ fuel cell employing Ti_{0.9}Mg_{0.1}P₂O₇/(Na/K)Ti₂(PO₄)₃ as electrolyte was fabricated.

Keywords: Fuel cells; *in-situ* reaction; Electrolyte; Conductivity

1. INTRODUCTION

Compared to fuel cells of low or high temperature, the fuel cells of intermediate temperature (300 °C ~ 800 °C) have many advantages. Exploring solid electrolyte materials which have high conductivity is key to the development of intermediate temperature fuel cells [1–7].

Over the past decade, TiP₂O₇-based electrolytes have been widely studied as intermediate temperature fuel cell electrolytes [8–12]. Lapina et al. researched the effect of sintering temperature and phosphorus content on the electrical conductivities of 10 mol % Y³⁺-doped titanium pyrophosphate [10]. Norby et al. synthesized Al³⁺-doped TiP₂O₇, and the isotope effect on conductivity showed that the sample had good protonic conduction [11]. More attractively, our previous work showed that Ti_{0.95}Mg_{0.05}P₂O₇ is an ionic conductor and has a high conductivity [12]. Unfortunately, the

single MP_2O_7 materials were impractical owing to their poor sintering abilities. The researchers have done a lot of research to overcome the shortcomings of MP_2O_7 single material [13–18]. For example, Hibino et al. prepared a dense H_3PO_4 -doped polybenzimidazole / $\text{Sn}_{0.95}\text{Al}_{0.05}\text{P}_2\text{O}_7$ composite electrolyte by *in-situ* reaction [15].

Many studies have shown that titanium phosphate has good alkali metal salt ion conductivity and high long-term stability in alkali metal salt ion batteries [19–24]. Whitacre et al. studied the long-term stability of $\text{NaTi}_2(\text{PO}_4)_3$ which was used as an anode material [19]. Xu et al. synthesized $\text{KTi}_2(\text{PO}_4)_3$ by a hydrothermal method. Moreover, a carbon-coated $\text{KTi}_2(\text{PO}_4)_3$ was obtained and it had high electrochemical performances in a sodium-ion battery [20]. In our previous work, we explored a titanium pyrophosphate/corresponding phosphate composite electrolyte [25]. The above researches indicate that pyrophosphate/corresponding phosphate material could overcome the poor mechanical strength of MP_2O_7 single material.

In this study, a new composite electrolyte of $(\text{Na/K})\text{Ti}_2(\text{PO}_4)_3/\text{Ti}_{0.9}\text{Mg}_{0.1}\text{P}_2\text{O}_7$ was synthesized using $\text{Ti}_{0.9}\text{Mg}_{0.1}\text{P}_2\text{O}_7$ and NaCl/KCl as raw materials. The characterization properties of the sample were carried out by SEM and XRD. The electrical conductivities of $(\text{Na/K})\text{Ti}_2(\text{PO}_4)_3/\text{Ti}_{0.9}\text{Mg}_{0.1}\text{P}_2\text{O}_7$ were studied at 300–700 °C. An intermediate temperature H_2/O_2 fuel cell was also fabricated.

2. EXPERIMENTAL

A $(\text{Na/K})\text{Ti}_2(\text{PO}_4)_3/\text{Ti}_{0.9}\text{Mg}_{0.1}\text{P}_2\text{O}_7$ was synthesized as follows. Reagent-grade MgO (0.24g), TiO_2 (4.32g) and 85 % H_3PO_4 (11.6mL) were used as raw materials to synthesize $\text{Ti}_{0.9}\text{Mg}_{0.1}\text{P}_2\text{O}_7$ [12]. Briefly, the raw materials were fully mixed and changed into a hard mud after heating at 350 °C for 1 h. $\text{Ti}_{0.9}\text{Mg}_{0.1}\text{P}_2\text{O}_7$ was obtained after the hard mud was grinded and calcined at 500 °C for 4 h. Then, NaCl/KCl (1:1 molar ratio) and $\text{Ti}_{0.9}\text{Mg}_{0.1}\text{P}_2\text{O}_7$ were mixed at a 1:4 weigh feed ratio and heated at 550 °C for 1.5 hours. After the complete reaction, the obtained powder was then heated at 600 °C for 1 h to get the $(\text{Na/K})\text{Ti}_2(\text{PO}_4)_3/\text{Ti}_{0.9}\text{Mg}_{0.1}\text{P}_2\text{O}_7$.

The crystallization of $(\text{Na/K})\text{Ti}_2(\text{PO}_4)_3/\text{Ti}_{0.9}\text{Mg}_{0.1}\text{P}_2\text{O}_7$ was tested by XRD. Surface and cross-sectional photos of the composite electrolyte were taken with SEM. To research the electrical conductivity of $(\text{Na/K})\text{Ti}_2(\text{PO}_4)_3/\text{Ti}_{0.9}\text{Mg}_{0.1}\text{P}_2\text{O}_7$, 80%Ag-20%Pd paste and Ag wire were used as electrode and current collector, respectively. The conductivity was measured by an electrochemical analyzer (CHI660E) in the frequency range of 1- 10^6 Hz in a dry nitrogen atmosphere at 300–700 °C. The composite electrolyte (diameter 18 mm, thickness 1.0 mm) was sealed between two alumina tubes by low melting glass ointment at 600 °C for 1 h. To research the ionic conduction under different $p\text{O}_2$, oxygen concentration cell and $\log\sigma$ as a function of $\log(p\text{O}_2)$ plot were measured in the range of the test temperatures [26]. The oxygen concentration cell was constructed: air, Pd-Ag | $(\text{Na/K})\text{Ti}_2(\text{PO}_4)_3/\text{Ti}_{0.9}\text{Mg}_{0.1}\text{P}_2\text{O}_7$ | Pd-Ag, O_2 at 400-700 °C. The H_2/O_2 fuel cell (H_2 , Pd-Ag | $(\text{Na/K})\text{Ti}_2(\text{PO}_4)_3/\text{Ti}_{0.9}\text{Mg}_{0.1}\text{P}_2\text{O}_7$ | Pd-Ag, O_2) of the composite electrolyte was also tested.

3. RESULTS AND DISCUSSION

Fig. 1 displays the crystal structure of the $(\text{Na/K})\text{Ti}_2(\text{PO}_4)_3/\text{Ti}_{0.9}\text{Mg}_{0.1}\text{P}_2\text{O}_7$. The peaks at 22.60° , 25.31° , 27.79° and 37.88° agree well with the purity phase of TiP_2O_7 (JCPDS 38-1468) [10–12]. The strongest diffraction peaks at 24.19° and 24.25° are assigned to $\text{KTi}_2(\text{PO}_4)_3$ (JCPDS 79-1880) and $\text{NaTi}_2(\text{PO}_4)_3$ (JCPDS 84-2012), respectively [19–20]. This seems to indicate that a reaction fully occurred to Mg^{2+} -doped titanium pyrophosphate and inorganic molten salt to form the $(\text{Na/K})\text{Ti}_2(\text{PO}_4)_3/\text{Ti}_{0.9}\text{Mg}_{0.1}\text{P}_2\text{O}_7$ [25].

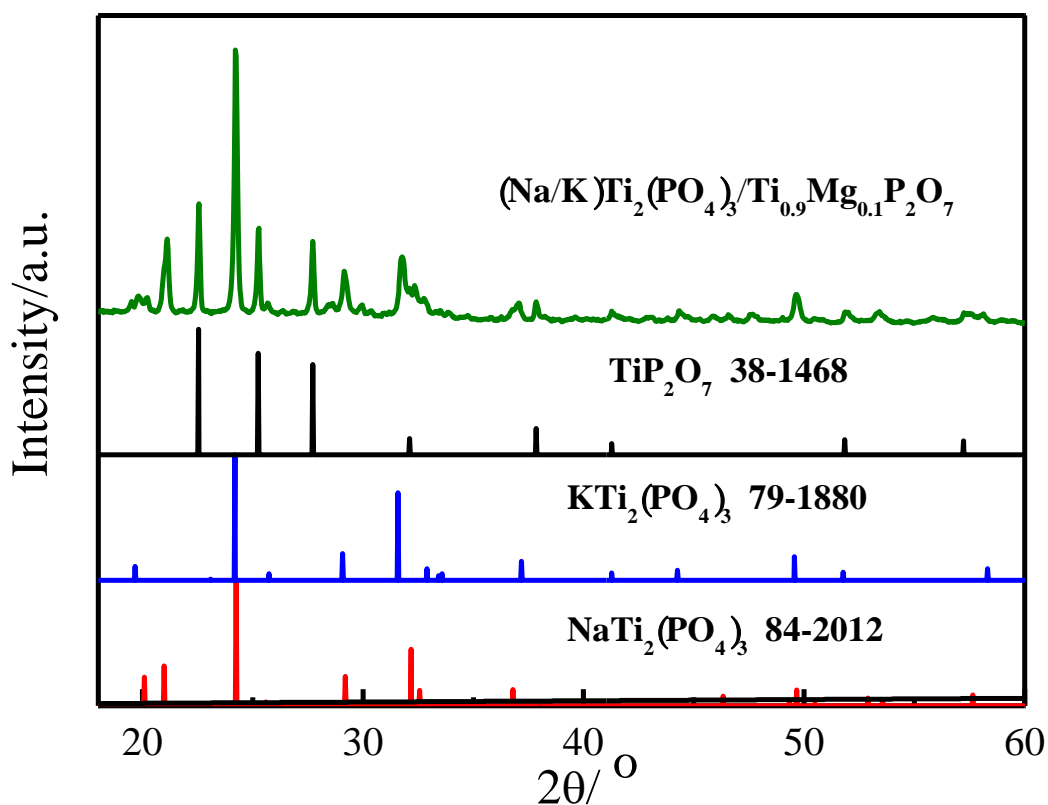


Figure 1. XRD pattern of $(\text{Na/K})\text{Ti}_2(\text{PO}_4)_3/\text{Ti}_{0.9}\text{Mg}_{0.1}\text{P}_2\text{O}_7$.

Fig. 2 displays the SEM photos which showed the external and cross-sectional surfaces of the $(\text{Na/K})\text{Ti}_2(\text{PO}_4)_3/\text{Ti}_{0.9}\text{Mg}_{0.1}\text{P}_2\text{O}_7$. In Fig. 2(a), the external surface of the $(\text{Na/K})\text{Ti}_2(\text{PO}_4)_3/\text{Ti}_{0.9}\text{Mg}_{0.1}\text{P}_2\text{O}_7$ exhibits an approximate cubic shape, and the solid surface is adequately covered by a fused layer. In Fig. 2(b), the cross-sectional surface has a small number of holes, however, the experimental test proved that they are closed holes [25].

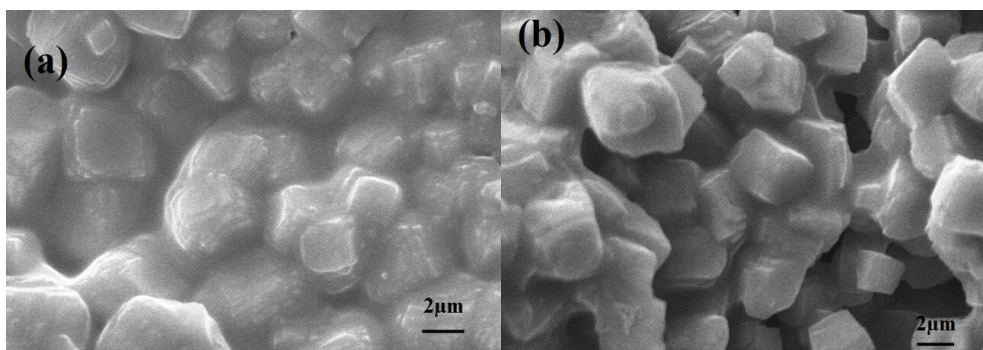


Figure 2. The SEM photos of the $(\text{Na/K})\text{Ti}_2(\text{PO}_4)_3/\text{Ti}_{0.9}\text{Mg}_{0.1}\text{P}_2\text{O}_7$ (a, b).

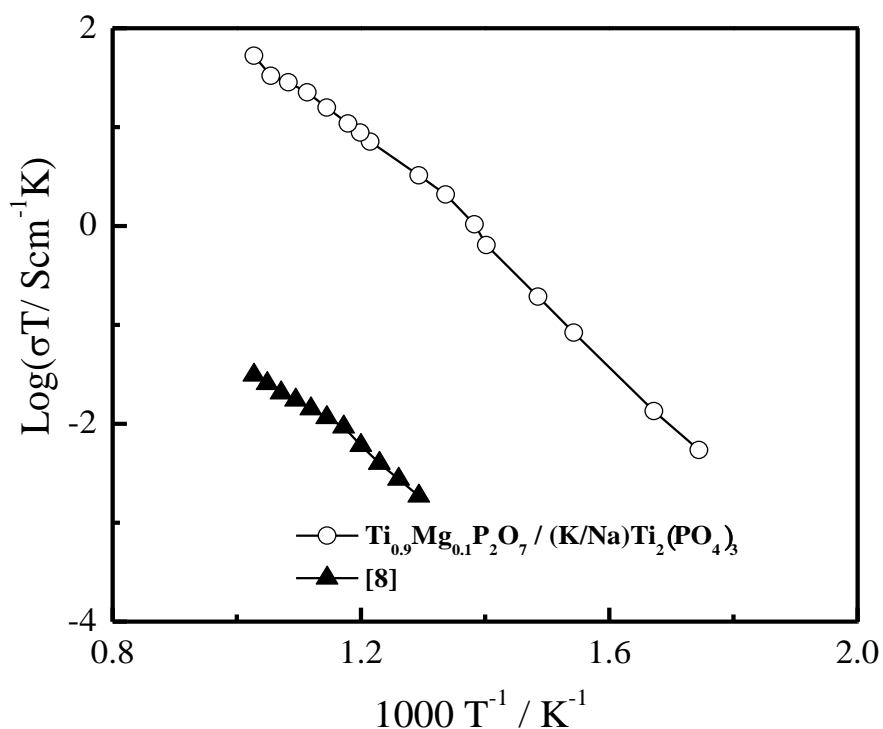


Figure 3. The plot of $\log(\sigma T) \sim 1000 T^{-1}$ of $(\text{Na/K})\text{Ti}_2(\text{PO}_4)_3/\text{Ti}_{0.9}\text{Mg}_{0.1}\text{P}_2\text{O}_7$ at 300–700 °C in dry nitrogen atmosphere.

According to the electrical conductivities of $(\text{Na/K})\text{Ti}_2(\text{PO}_4)_3/\text{Ti}_{0.9}\text{Mg}_{0.1}\text{P}_2\text{O}_7$ shown in Fig.3, as expected, the ionic conductivity of the sample increases with increasing test temperature and reaches the maximum ionic conductivity is $5.4 \times 10^{-2} \text{ S} \cdot \text{cm}^{-1}$ at 700 °C. Compare with the literature, the $(\text{Na/K})\text{Ti}_2(\text{PO}_4)_3/\text{Ti}_{0.9}\text{Mg}_{0.1}\text{P}_2\text{O}_7$ is about four orders of magnitude higher than low valence metal ion doped TiP_2O_7 [8]. It can be attributed to the phase structure (Fig. 1) and additional transport pathways for protons (Fig. 2) formed by titanium phosphate with NASICON structure [25].

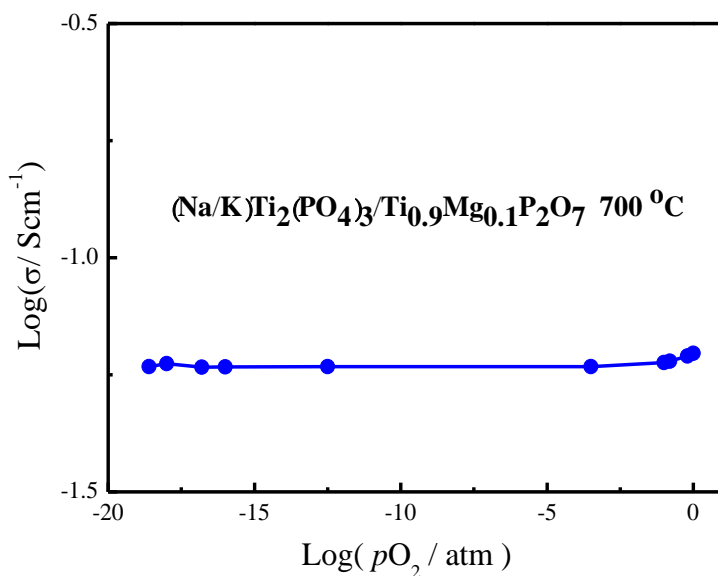


Figure 4. The $\log \sigma$ versus $\log(p\text{O}_2)$ plot of $(\text{Na/K})\text{Ti}_2(\text{PO}_4)_3/\text{Ti}_{0.9}\text{Mg}_{0.1}\text{P}_2\text{O}_7$ at 700 °C.

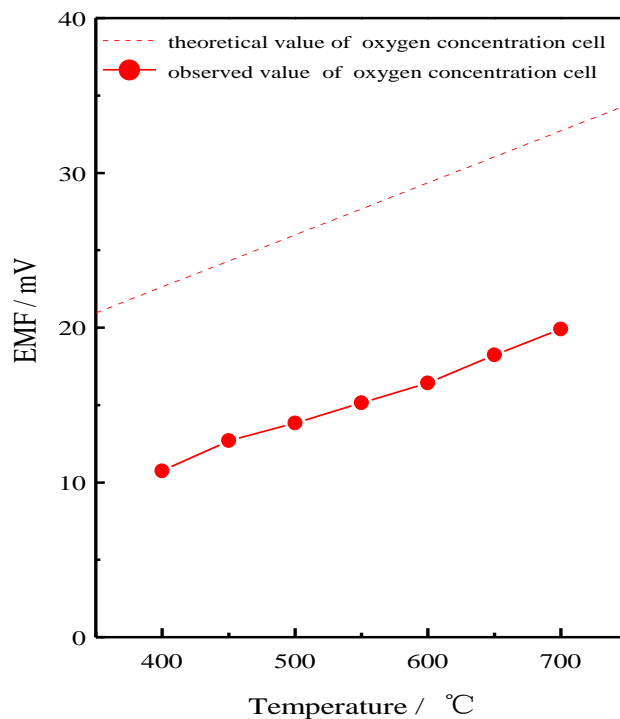


Figure 5. The relation between EMF and temperature of oxygen concentration cell: air, Pd-Ag | $(\text{Na/K})\text{Ti}_2(\text{PO}_4)_3/\text{Ti}_{0.9}\text{Mg}_{0.1}\text{P}_2\text{O}_7$ | Pd-Ag, O_2 .

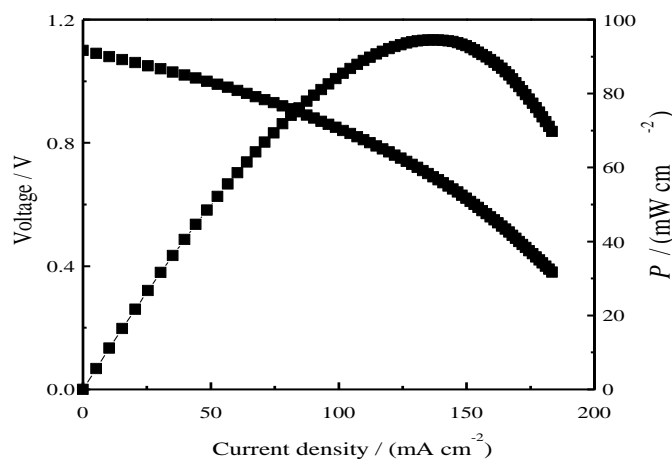


Figure 6. The H₂/O₂ fuel cell *I-V-P* curve of (Na/K)Ti₂(PO₄)₃/Ti_{0.9}Mg_{0.1}P₂O₇ at 700 °C.

The $\log \sigma \sim \log(pO_2)$ plot of (Na/K)Ti₂(PO₄)₃/Ti_{0.9}Mg_{0.1}P₂O₇ represented in Fig. 4, was used to study the ionic conduction at 700 °C. The left half of Fig. 4 is horizontal in a reductive atmosphere ($10^{-20} \sim 10^{-10}$ atm), which confirms that (Na/K)Ti₂(PO₄)₃/Ti_{0.9}Mg_{0.1}P₂O₇ is a good ionic conductor [26]. Meanwhile, the right half of Fig. 4 is upwards as the pO_2 increases, which means (Na/K)Ti₂(PO₄)₃/Ti_{0.9}Mg_{0.1}P₂O₇ is a mixed conductor of electron hole and oxide ion in a oxidizing atmosphere ($10^{-10} \sim 10^0$ atm) [27-28].

To study the oxide ionic conduction of (Na/K)Ti₂(PO₄)₃/Ti_{0.9}Mg_{0.1}P₂O₇ in a oxidizing atmosphere, an oxygen concentration cell was devised and the results are displayed in Fig.5. The oxide ionic transport numbers (t_O) could be calculated on the basis of $t_O = EMF_{obs} / EMF_{cal} = 0.47-0.61$. The EMF_{cal} and EMF_{obs} are the theoretical and observed electromotive forces of the oxygen concentration cell, respectively. The EMF_{cal} is calculated as: $EMF_{cal} = \frac{RT}{4F} t_O \ln[pO_2(A) / pO_2(B)]$ when $t_O = 1$. The results are agreed with the right half of Fig. 4 ($10^{-10} \sim 10^0$ atm) and prove that electron hole conduction exists besides the oxide ionic conduction.

Fig. 6 shows the *I-V-P* characteristics of (Na/K)Ti₂(PO₄)₃/Ti_{0.9}Mg_{0.1}P₂O₇. Fig. 6 shows that the voltage is about 1.1 V which indicates there is no crossover of H₂ or O₂. The peak power output density of the (Na/K)Ti₂(PO₄)₃/Ti_{0.9}Mg_{0.1}P₂O₇ (thickness = 1.0 mm) is 94.5 mW·cm⁻² at 700 °C. Chen et al. got a peak power density of 17.3 mW·cm⁻² at 700 °C using Sn_{0.9}In_{0.1}P₂O₇ as electrolyte (thickness = 0.78 mm) [29]. Compared with the MP₂O₇-based single electrolytes, the (Na/K)Ti₂(PO₄)₃/Ti_{0.9}Mg_{0.1}P₂O₇ not only improves fuel cell performance, but also increases the application temperature range.

4. CONCLUSIONS

In this paper, a novel composite electrolyte of (Na/K)Ti₂(PO₄)₃/Ti_{0.9}Mg_{0.1}P₂O₇ was successfully synthesized by a one-step approach using Mg²⁺-doped titanium pyrophosphate and inorganic molten salt as precursors. The SEM results demonstrated that two phases of Ti_{0.9}Mg_{0.1}P₂O₇ and corresponding phosphate, (Na/K)Ti₂(PO₄)₃, are interconnected a dense electrolyte. The highest conductivity of the

composite electrolyte was $5.4 \times 10^{-2} \text{ S} \cdot \text{cm}^{-1}$ in dry N_2 at $700 \text{ }^\circ\text{C}$. The results of electrical conductivity measurement and $\log \sigma \sim \log(p\text{O}_2)$ plot show that $(\text{Na/K})\text{Ti}_2(\text{PO}_4)_3/\text{Ti}_{0.9}\text{Mg}_{0.1}\text{P}_2\text{O}_7$ is a mixed conductor of oxide ions and electron holes in an oxidizing atmosphere and an ionic conductor in a reductive atmosphere. The peak power output density of the composite electrolyte reached $94.5 \text{ mW} \cdot \text{cm}^{-2}$ at $700 \text{ }^\circ\text{C}$.

ACKNOWLEDGEMENTS

This work was supported by the National Natural Science Foundation (No. 51402052) of China. The Provincial Natural Science Research Project of Anhui Colleges (No. 2015KJ005, KJ2018A0337, KJ2018A0980). Excellent Youth Foundation of Anhui Educational Committee (No. gxyq2018046). Horizontal cooperation project of Fuyang municipal government and Fuyang Normal College (No. XDHX2016019).

References

1. J. Luo, A.H. Jensen, N.R. Brooks, J. Sniekers, M. Knipper, D. Aili, Q. Li, B. Vanroy, M. Wübbenhorst, F. Yan, L.V. Meervelt, Z. Shao, J. Fang, Z.-H. Luo, D.E.D. Vos, K. Binnemans and J. Fransaer, *Energy Environ. Sci.*, 8(2015) 1276.
2. X. Gao, J. Ma, Y. Li and H. Wei, *Int. J. Electrochem. Sci.*, 12 (2017) 11287.
3. T. Hibino, K. Kobayashi, P. Lv, M. Nagao, S. Teranishi and T. Mori, *J. Electrochem. Soc.*, 164 (2017) F557.
4. K. K. Hansen, *Int. J. Electrochem. Sci.*, 12 (2017) 11540.
5. T. Hibino, K. Kobayashi, M. Nagao and S. Teranishi, *ChemElectroChem*, 4 (2017) 3032.
6. O. K. Alekseeva, E. K. Lutikova, V. V. Markelov, V. I. Poremsky and V. N. Fateev, *Int. J. Electrochem. Sci.*, 13 (2018) 797.
7. X. Zhang, J. Luo, P. Tang, J. R. Morante, J. Arbiol, C. Xu, Q. Li and J. Fransaer, *Sens. Actuators B Chem.*, 254 (2018) 272.
8. V. Nalini, M. H. Sorby, K. Amezawa, R. Haugrud, H. Fjellvag and T. Norby, *J. Am. Ceram. Soc.*, 94 (2011) 1514.
9. B. Singh, H. N. Im, J. Y. Park and S. J. Song, *J. Phys. Chem. C*, 117 (2013) 2653.
10. A. Lapina, C. Chatzichristodoulou, J. Hallinder, P. Holtappels and M. Mogensen, *J. Solid State Electrochem.*, 18 (2014) 39.
11. V. Nalini, R. Haugrud and T. Norby, *Solid State Ionics*, 181 (2010) 510.
12. H. Wang, L. Sun, C. Luo, R. Yin and Y. Cui, *Ceram. Int.*, 41 (2015) 2124.
13. Y. Sato, Y.B. Shen, M. Nishida, W. Kanematsu and T. Hibino, *J. Mater. Chem.*, 22 (2012) 3973.
14. B. Singh, J. H. Kim, O. Parkash and S. J. Song, *Ceram. Int.*, 42 (2016) 2983.
15. Y.C. Jin, M. Nishida, W. Kanematsu and T. Hibino, *J. Power Sources*, 196 (2011) 6042.
16. P. Heo, Y. Shen, K. Kojima, C. Pak, K. H. Choi and T. Hibino, *Electrochim. Acta*, 128 (2014) 287.
17. Q. Li, H. A. Hjuler and N. J. Bjerrum, *J. Appl. Electrochem.*, 31 (2001) 773.
18. J. Liao, J. Yang, Q. Li, L. N. Cleemann, J. O. Jensen, N. J. Bjerrum, R. He and W. Xing, *J. Power Sources*, 238 (2013) 516.
19. A. I. Mohamed and J. F. Whitacre, *Electrochim. Acta*, 235 (2017) 730.
20. J. Han, M. Xu, Y. Niu, M. Jia, T. Liu and C. M. Li, *Journal of Colloid and Interface Science*, 483 (2016) 67.
21. N. Li, Y. Wang, R. Rao, X. Dong, X. Zhang and S. Zhu, *Applied Surface Science*, 399 (2017) 624.
22. M. Bian and L. Tian, *Ceram. Int.*, 43 (2017) 9543.
23. H.J. Zhang, *Acta Cryst.*, E67 (2011) i51.

24. P. Hu, J. Ma and T. Wang, *Chem. Mater.*, 27 (2015) 6668.
25. R. Shi, R. Du, J. Liu and Hongtao Wang, *Ceram. Int.*, 44 (2018) 11878.
26. J. Guan, S.E. Dorris, U. Balachandran and M. Liu, *Solid State Ion.*, 100 (1997) 45.
27. G. Ma, T. Shimura and H. Iwahara, *Solid State Ion.*, 120 (1999) 51.
28. N. Sammes, R. Phillips and A. Smirnova, *J. Power Sources*, 134 (2004) 153.
29. X. Chen, C. Wang, E. A. Payzant, C. Xia and D. Chu, *J. Electrochem. Soc.*, 155 (2008) B1264.

© 2018 The Authors. Published by ESG (www.electrochemsci.org). This article is an open access article distributed under the terms and conditions of the Creative Commons Attribution license (<http://creativecommons.org/licenses/by/4.0/>).